

Biaxial Buckling of Single-Layer Graphene Sheet Based on Nonlocal Plate Model and Molecular Dynamics Simulation

R. Pilafkan* M. Kaffash Mirzarahimi

Department of Engineering, University of Mohaghegh Ardabili, Ardabil, Iran

Abstract

This paper considers biaxial buckling behavior of single-layered graphene sheets (SLGSs) using molecular dynamics (MD) and nonlocal elasticity theory. Based on the MD simulations, Large-scale Atomic/Molecular Massively Parallel Simulator (LAMMPS), an open source software, is used to obtain critical buckling loads. On the other hand, governing equations are derived using nonlocal elasticity and classical plate theory (CLPT) and solved using generalized differential quadrature method (GDQ). The small-scale effect is applied in governing equations of motion by nonlocal parameter. The effect of different side lengths, boundary conditions and nonlocal parameter are inspected for aforementioned methods. Results are obtained from MD simulations is compared with those of the nonlocal elasticity theory to calculate appropriate values for the nonlocal parameter. The nonlocal parameter value is suggested for graphene sheets with various boundary conditions.

Article history

Received: 2018-04-18

Revised: 2018-07-28

Accepted: 2018-08-15

Keywords

Biaxial buckling
Single-layered graphene sheets
Nonlocal elasticity
Molecular dynamics simulation
Classical plate theory

1. Introduction

Due to outstanding mechanical, electrical, and chemical properties, the families of carbon nanostructures such as graphene sheets, carbon nanotubes, and fullerenes provide a new foundation to apply in different emerging fields of nanoscience and nanotechnology [1-4]. Different kinds of graphene sheets conformation are shown in Fig. 1. Because of their small scale, there are some difficulties in conducting experiments to investigate the behaviors of nanostructures which make their theoretical analyses become increasingly important.

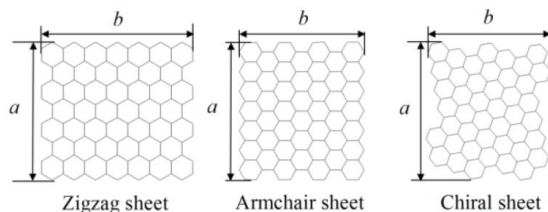


Fig. 1. Chirality and geometrical parameters of single-layered graphene sheets.

Based on the classical plate theory (CLPT), Kitipornchai et al. [5] investigated the vibration response of multi-layered

graphene sheets (MLGSs) with simply-supported boundary conditions using a continuum model. They proposed an explicit formula for the van der Waals interaction between any two sheets of an MLSG. Liew and his coworkers [6] proposed a continuum model to analyze the vibrations of MLSG embedded in an elastic matrix.

As the classical continuum models do not have the capability to consider the size-effects in the analysis of nanostructures, using them to predict the behavior of structures at the nanoscale becomes controversial. Hence, the extension of the continuum mechanics to accommodate the size dependence of nanostructures is a topic of major concern. Modified continuum models are one of the most applied theoretical approaches for the investigation of nanomechanics due to their computational efficiency and their capability to produce accurate results which are comparable to those of the atomistic models [4]. The application of nonlocal continuum mechanics allowing for the small scale effects in the analysis of nanostructures has been recommended by many research workers.

Ansari et al. [7] developed a nonlocal finite element model to investigate the vibrations of MLGSs with different boundary conditions embedded in an elastic medium. Shen and his assistances [8] studied the nonlinear vibrations of simply supported SLGSs in thermal environment based on nonlocal orthotropic plate model. The vibration analysis of MLGSs embedded in a polymer matrix was investigated by Pradhan and Phadikar [9] using nonlocal continuum mechanics.

Continuing with the nonlocal continuum applications, Murmu and Pradhan [10] developed a single-elastic beam model to analyze the thermal vibration of CNTs based on thermal elasticity mechanics, and nonlocal elasticity theory. nonlocal scale parameter effects on the wave propagation in multi-walled carbon nanotubes was represented by Narendar and Gopalakrishnan [11]. Arash and Ansari [12] studied the vibration characteristics of single-walled carbon nanotubes (SWCNTs) based upon a nonlocal shell model. There are so many other researches in which the behaviors of nanostructures under various loading conditions have been predicted based on continuum elastic models [13–15] which indicates the wide range of application of this type of modified continuum mechanics in the nanomechanics.

2. Stress state characterization

The essence of the nonlocal elasticity theory is that the stress field at a reference point x in an elastic continuum depends not only on strain at that point but also on strains at all other points in the body. This is in accordance with the atomic theory of lattice dynamics and experimental observations on phonon dispersion. The scale effects are accounted for in the theory by considering internal size as a material parameter. The most general form of the constitutive relation for nonlocal elasticity involves an integral over the whole body. According to the nonlocal elasticity theory initiated by Eringen [16], the nonlocal constitutive equation in differential form can be written as:

$$(1 - \mu \nabla^2) \sigma = S : \varepsilon \tag{1}$$

where S is the fourth order elasticity tensor and ‘:’ denotes the double dot product, σ is nonlocal stress tensor and ε is strain tensor. μ

is a material constant ($\mu = e_0 a / l$) that depends on the internal (lattice parameter, granular size, distance between C–C bonds), a and external characteristics lengths (crack length, wave length), l . The parameter e_0 is estimated such that the relations of the non-local elasticity model could provide satisfied approximation of atomic dispersion curves of plane waves with those of atomic lattice dynamics. ∇^2 is the Laplacian operator which is given by $(\partial^2 / \partial x^2 + \partial^2 / \partial y^2)$. Two-dimensional nonlocal constitutive relations can be expressed as

$$\begin{Bmatrix} \sigma_{xx} \\ \sigma_{yy} \\ \sigma_{xy} \end{Bmatrix} - \mu \nabla^2 \begin{Bmatrix} \sigma_{xx} \\ \sigma_{yy} \\ \sigma_{xy} \end{Bmatrix} = \begin{bmatrix} E / (1 - \nu^2) & \nu E / (1 - \nu^2) & 0 \\ \nu E / (1 - \nu^2) & E / (1 - \nu^2) & 0 \\ 0 & 0 & E / 2(1 + \nu) \end{bmatrix} \begin{Bmatrix} \varepsilon_{xx} \\ \varepsilon_{yy} \\ \varepsilon_{xy} \end{Bmatrix} \tag{2}$$

here E is the Young’s modulus of the material and ν is the Poisson ratio. To model the SLGSs, consider a thin elastic plate of length a in the x -direction, width b in the y -direction and thickness h , as shown in Fig. 2. Based on the classical plate theory, the displacement components (u_1, u_2, u_3) along the axes (x, y, z) can be written in a general form as:

$$u_1 = -z \frac{\partial w}{\partial x}; u_2 = -z \frac{\partial w}{\partial y}; u_3 = w(x, y, t) \tag{3}$$

where w is the lateral deflection.

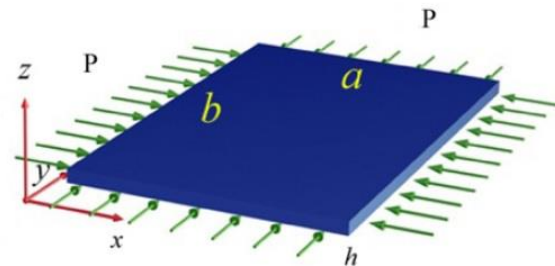


Fig.2 Schematic of a biaxially compressed monolayer GS.

where P is the critical biaxial buckling load. The bending and twisting moments per unit length are given by:

$$\{M_{xx}, M_{yy}, M_{xy}\}^T = \int_{-h/2}^{h/2} z \{\sigma_{xx}, \sigma_{yy}, \sigma_{xy}\}^T dz \tag{4}$$

With the principle of virtual work, the equilibrium equation governing the buckling of biaxially compressed plates takes the form:

$$\frac{\partial^2 M_{xx}}{\partial x^2} + \frac{\partial^2 M_{yy}}{\partial y^2} + 2 \frac{\partial^2 M_{xy}}{\partial x \partial y} - P \left(\frac{\partial^2 w}{\partial x^2} + \frac{\partial^2 w}{\partial y^2} \right) = 0 \tag{5}$$

Using Eqs. (2) and (4), one can arrive at the nonlocal governing equation of (5) in terms of displacements as

$$-\frac{Eh^3}{12(1-\nu^2)}\left(\frac{\partial^4 w}{\partial x^4} + \frac{\partial^4 w}{\partial y^4} + 2\nu\frac{\partial^4 w}{\partial x^2\partial y^2}\right) - \frac{Eh^3}{6(1+\nu)}\frac{\partial^4 w}{\partial x^2\partial y^2} \quad (6)$$

$$-P\left(\frac{\partial^2 w}{\partial x^2} + \frac{\partial^2 w}{\partial y^2}\right) = 0$$

3. GDQM solution procedure

The DQ method has been proved to be an efficient higher-order numerical technique for the solution of initial and boundary value problems. The DQ technique has been widely reported to yield successful solutions for various dynamic and stability problems [15-16].

The m th-order derivative of a single function $f(x)$ at a given discrete grid point i can be approximated by the DQ method with N discrete grid points as:

$$\left.\frac{\partial^m f(x_i, y_j)}{\partial x^m}\right|_{(x_i, y_j)} = \sum_{j=1}^N w_{ij}^{(m)} f(x_j, y_k); \quad i = 1, 2, \dots, N \quad (7)$$

where N is the number of grid points in the x -direction and $w_{ij}^{(m)}$ represents the respective weighting coefficient related to the m th-order derivative. So, for example, if $m = 1$, the first-order derivative is obtained as follows:

$$w_{ik}^{(1)} = \frac{\prod_{k=1, k \neq i}^N (x_i - x_k)}{(x_i - x_j) \prod_{k=1, k \neq j}^N (x_j - x_k)}; \quad i, j = 1, 2, \dots, N, \quad i \neq j \quad (8)$$

$$w_{ii}^{(1)} = -\sum_{i=1, j \neq i}^N w_{ij}^{(1)}; \quad i = 1, 2, \dots, N$$

where the superscript (m) and $(m+1)$ denote the order of the derivative. The number of discrete grid points and the grid point distribution can be chosen arbitrarily in the implementation of the DQM. However, it is shown that the grid point distribution, which is based on well-accepted Gauss-Chebyshev-Lobatto points [17], gives sufficiently accurate results. The coordinates of the grid points are as follows:

$$x_i = a \frac{1 - \cos[(i-2)\pi/(N-3)]}{2}; \quad i = 3, 4, \dots, N-2; \quad (9)$$

$$x_1 = 0, \quad x_2 = a\delta, \quad x_N = a, \quad x_{N-1} = a - a\delta, \quad \delta = 1 \times 10^{-5}$$

$$y_j = a \frac{1 - \cos[(j-2)\pi/(M-3)]}{2}; \quad j = 3, 4, \dots, M-2; \quad (10)$$

$$y_1 = 0, \quad y_2 = b\delta, \quad y_M = b, \quad y_{M-1} = b - b\delta, \quad \delta = 1 \times 10^{-5}$$

where N is the number of grid points in the y -direction and M is the number of grid points in the x -direction. In the case of the rectangular graphene sheet, the computational domain is

$0 \leq x \leq a$ and $0 \leq y \leq b$. In the present case same numbers of grid points are used in x and y -directions ($N=M$). As it was previously mentioned, a and b are the length and width of the graphene sheet, respectively. Here, it is assumed that the thickness of the plate is constant. GDQM can be used to deal with complicated problems reasonably well because its implementation is very simple.

For convenience and generality Eq (6) we introduce the following nondimensional parameters:

$$W = w/a, \quad \xi = x/a, \quad \eta = y/b, \quad \mu = e_0 a / l \quad (11)$$

$$\beta = a/b, \quad \bar{N}^0 = \frac{PL^3}{D}, \quad \psi = \frac{e_0 a}{a}, \quad D = \frac{Eh^3}{12(1-\nu^2)}$$

Substituting Eq. (11) into Eq. (6), we have the nonlocal governing equation for compressed plate in nondimensional form:

$$\left(\frac{\partial^4 W}{\partial \xi^4} + \frac{\partial^4 W}{\partial \eta^4} + 2\beta^2 \frac{\partial^4 W}{\partial \xi^2 \partial \eta^2}\right) \quad (12)$$

$$+ \bar{N}^0 \psi^2 \left\{ \left(\frac{\partial^4 W}{\partial \xi^4} + \mu\beta^4 \frac{\partial^4 W}{\partial \eta^4} + (\mu+1)\beta^2 \frac{\partial^4 W}{\partial \xi^2 \partial \eta^2}\right) \right\}$$

$$- \bar{N}^0 \psi^2 \left(\frac{\partial^2 W}{\partial \xi^2} + \mu\beta^2 \frac{\partial^2 W}{\partial \eta^2}\right) = 0$$

Transformation of continuous boundary conditions into discretized form under GDQ rule mapping is performed by a direct substitution of these conditions into governing equations, as shown in [18]:

All edges simply supported (SSSS):

$$W = 0, \quad \sum_{m=1}^{N_x} B_{jm}^{(2)} W_{im}; \quad i = 1, N_x; \quad \text{At } x=0, x=a \quad (13)$$

$$W = 0, \quad \sum_{k=1}^{N_y} A_{ik}^{(2)} W_{kj}; \quad j = 1, N_y; \quad \text{At } y=0, y=b$$

All edges clamped (CCCC):

$$W = 0, \quad \sum_{m=1}^{N_x} B_{jm}^{(1)} W_{im}; \quad i = 1, N_x; \quad \text{At } x=0, x=a \quad (14)$$

$$W = 0, \quad \sum_{k=1}^{N_y} A_{ik}^{(1)} W_{kj}; \quad j = 1, N_y; \quad \text{At } y=0, y=b$$

Two opposite long edges simply supported, others clamped

(CCSS):

$$W = 0, \quad \sum_{m=1}^{N_x} B_{jm}^{(1)} W_{im}; \quad i = 1, N_x; \quad \text{At } x=0, x=a \quad (15)$$

$$W = 0, \quad \sum_{k=1}^{N_y} A_{ik}^{(2)} W_{kj}; \quad j = 1, N_y; \quad \text{At } y=0, y=b$$

The computational domain of the rectangular plate is $0 \leq \xi \leq 1$; $0 \leq \eta \leq 1$. Making use of Eq. (7) and incorporating the boundary conditions by modified weighting coefficient method [18] we write Eq. (12) in nondimensional form:

$$\begin{aligned}
& \left(\sum_{k=2}^{N_x-1} A_{ik}^{(4)} W_{kj} + 2\beta^2 \sum_{k=2}^{N_x-1} \sum_{m=1}^{N_x-1} A_{ik}^{(2)} B_{jm}^{(2)} W_{km} + \beta^4 \sum_{m=1}^{N_x} B_{jm}^{(4)} W_{im} \right) \\
& + \bar{N}^0 \left[\psi^2 \left(\sum_{k=2}^{N_x-1} A_{ik}^{(4)} W_{kj} + 2\beta^2 \sum_{k=2}^{N_x-1} \sum_{m=1}^{N_x-1} A_{ik}^{(2)} B_{jm}^{(2)} W_{km} + \beta^4 \sum_{m=1}^{N_x} B_{jm}^{(4)} W_{im} \right) \right. \\
& \left. - \left(\sum_{k=2}^{N_x-1} A_{ik}^{(2)} W_{kj} + \beta^2 \sum_{m=1}^{N_x} B_{jm}^{(2)} W_{im} \right) \right] = 0
\end{aligned} \tag{16}$$

It should be noted that the Eq. (18) is solved for inner grid

points. DQ procedures could be advantageous in dealing with nonlocal elasticity problems of small scale structures over other approaches because its implementation is very simple and could handle complicated problems reasonably well. These problems include nonlocal Mindlin plate theory or higher order nonlocal plate theories with axially stressed conditions. The above DQ analogous (Eq. (16)) can easily be reduced to an eigenvalue problem:

$$[K]_{total} \{W\} = \bar{N}^0 \{W\} \tag{17}$$

where \bar{N}^0 is the nondimensional buckling load described in Eq. (11). The Eq. (17) can be solved by a standard eigenvalue solver. From this solution the buckling loads of graphene sheets are obtained.

4. Modeling and simulation

Square zigzag graphene sheets are considered in this study. The definitions of the chirality for the graphene sheets are similarly defined as in carbon nano-tubes [19, 20]. The boundary conditions of the graphene sheets are assumed to be SSSS, CCCC and CCSS.

The parallel molecular dynamics code package LAMMPS [21] is used for performing the MD simulations, while the molecular visualization package VMD [22] is employed for post-processing of the simulation results.

In the MD simulations, energy minimization is first conducted to fully relax the system with free boundary.

All simulations are established using the Adaptive Intermolecular Reactive Empirical Bond Order (AIREBO) potential [23]. The AIREBO potential is an extension of the commonly used REBO potential developed for solid carbon and hydrocarbon molecules [24].

There are various factors which can significantly affect the results obtained from MD simulations. The most important ones are thermal conditions, time step, and strain rate. The MD simulations presented here are all

performed at constant temperature equal to the room temperature (I.e., a canonical NVT ensemble). The van Gunsteren–Berendsen thermostat [25] is employed in such a way that the scaling factor is used after each step of the MD simulation; the velocities of the atoms of system are scaled as the average kinetic energy remains approximately constant. To choose the value of time step, on the basis of a general rule, it should be smaller than one-tenth of the vibration period time for an atom of the system simulated by MD simulation [26].

Based on the obtained stress and strain history, we can plot the stress–strain curve to investigate the mechanical behavior under compression. The point where the elastic response ends is defined as the onset of buckling, the corresponding strain is referred to as the critical strain.

An algorithm containing the summary of procedure conducted in the MD simulations is shown in Fig. 3. Compressive biaxial strain is applied to the all sides of each SLGS by mathematically changing the coordinates of the carbon atoms [4] to a biaxial compressively strained condition. Then using the LAMPPS simulator, various time steps to relax the system of atoms to their equilibrium position are arranged to enable the nanosheets reach to the equilibrium configuration. This procedure is repeated for different values of the compressive strain while for a certain value of the strain, the SLGS collapses corresponding to its buckling mode shape as depicted in Fig. 4.

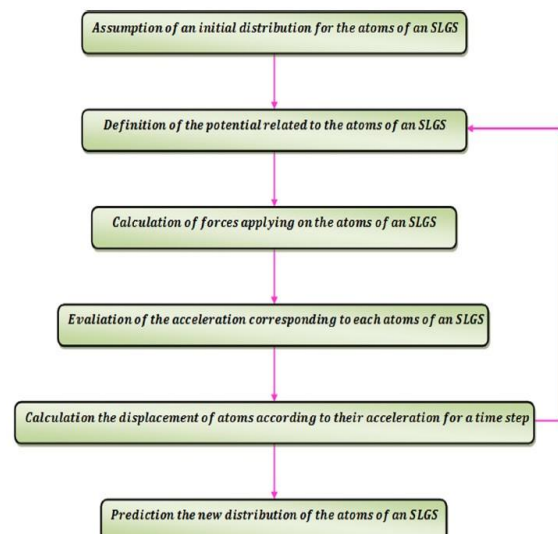


Fig. 3. Algorithm of an MD simulation

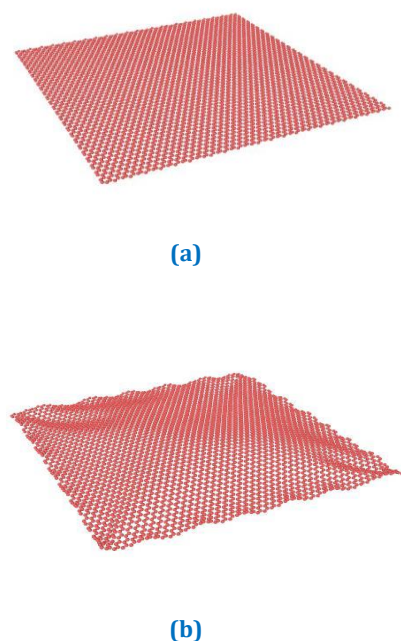


Fig. 4. An SLGS under biaxial compressive strain (a) simulation start, (b) after relaxation.

4. Results and Discussion

The thickness of plate in the nonlocal plate elasticity models is assumed to be equal to the spacing of graphite ($h = 0.34$ nm). Moreover, the values of Young's modulus and Poisson's ratio are considered $E = 1$ TPa and $m = 0.16$, respectively [26].

In order to assess the accuracy of the present study, the critical biaxial buckling loads of square armchair monolayer GSs with all edges simply supported obtained via Eq. (17) by GDQM are compared with those of MD simulations in Table 1 for different values of side length. The nonlocal parameter μ is calculated by utilizing the least square technique so that the sum of the squares of the errors between the results from MD simulations and the corresponding ones from the present model is minimized. The least squares method is a form of mathematical regression analysis that finds the line of best fit for a dataset, providing a visual demonstration of the relationship between the data points. Each point of data is representative of the relationship between a known independent variable and an unknown dependent variable. [27]. It is observed that the two sets of results are in excellent agreement. Therefore, the nonlocal formulas given by Eq.

(17) can be considered as reliable relations capable of determination of critical biaxial buckling loads of SLGS provided that the nonlocal parameter is properly calibrated.

Table 1. MD and gdqm results for critical biaxial buckling loads of simply-supported zigzag square SLGSs (nN).

Side lengths (nm)	MD	GDQM($\mu=1.86$ nm ²)	Error%
4.99	1.0835	1.1219	3.5
8.08	0.6535	0.6524	0.1
10.077	0.4459	0.4412	1.0
14.65	0.2609	0.2685	2.9
22.35	0.1191	0.1228	3.0
30.04	0.0737	0.0714	3.2
37.81	0.0449	0.0456	1.5

Influence of the nonlocal parameter (e_0a) and the side length on the critical biaxial buckling loads is investigated in Fig. 5 for the SSSS boundary conditions and Fig. 6 and Fig. 7 illustrate similar curves for the CCCC and SCSC boundary conditions, respectively. As shown in these figures the critical biaxial buckling loads declines substantially with increase in the nonlocal parameter, for the side smaller than 30 nm because of the small-scale effect. However for the larger SLGSs nonlocal parameter has a negligible impact on the critical biaxial buckling loads, as expected. Therefore the local forms of governing equations can be applied to the graphene sheets with larger sides without causing noticeable error. Also, it can be observed that the lower critical biaxial buckling loads is obtained for the higher length of square. Further, one can notice from these figures that increasing constraints results in the critical biaxial buckling loads. Therefore, for the equal side lengths and nonlocal parameter values critical biaxial buckling loads corresponding to CCCC boundaries are higher than those of SCSC boundaries and those of to SCSC are higher than one's corresponding to the SSSS boundaries.

Table 2 presents the appropriate values of μ derived through fitting procedure corresponding to different types of boundary conditions. It is evident that there is an excellent agreement between the results of MD simulations and the ones predicted by the

present nonlocal continuum plate model with their appropriate values of nonlocal parameter.

Table 2. appropriate values of nonlocal parameter corresponding to different types of boundary conditions

Type of boundary conditions	Appropriate value of nonlocal parameter(e_0a)
SSSS	1.86
CCCC	1.17
CCSS	1.52

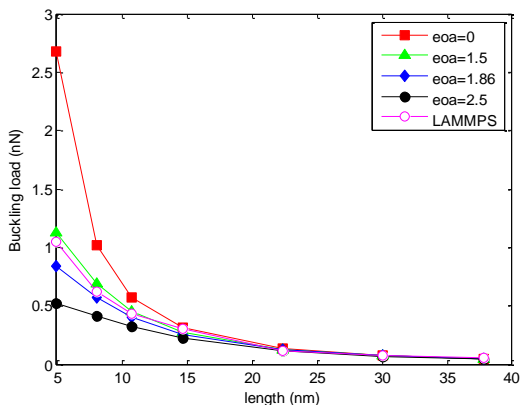


Fig. 5. Variation of critical biaxial buckling load with side-length of square SLGS corresponding to the different values of nonlocal parameter for nonlocal CLPT and comparison with MD simulation for SSSS.

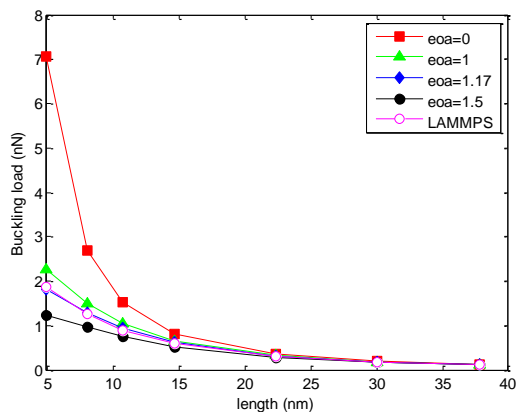


Fig. 6. Variation of critical biaxial buckling load with side-length of square SLGS corresponding to the different values of nonlocal parameter for nonlocal CLPT and comparison with MD simulation for CCCC.

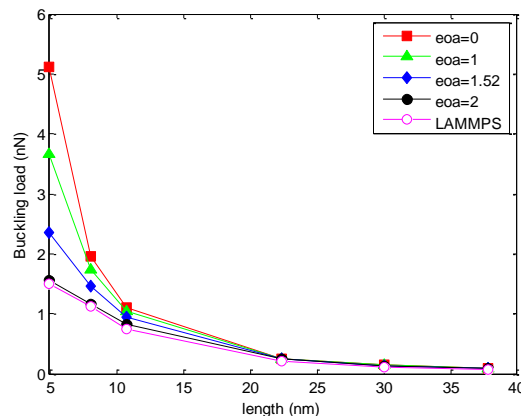


Fig. 7. Variation of critical biaxial buckling load with side-length of square SLGS corresponding to the different values of nonlocal parameter for nonlocal CLPT and comparison with MD simulation for CCSS.

5. Conclusion

Biaxial buckling characteristics of SLGSs were investigated in this work. To this end, Eringen’s nonlocal elasticity equations were incorporated into classical plate theory (CLPT) to consider the size-effects in the biaxial analysis. GDQM form of numerically solution was conducted to obtain the critical biaxial buckling loads of SSSS, CCCC and CCSS square SLGSs with different values of side-length and nonlocal parameter.

Afterward, MD simulations were performed for zigzag SLGSs with different values of side-length, and boundary conditions the results of which were fitted with those calculated by the nonlocal elasticity plate model through a least-square fitting procedure to extract the correct values of nonlocal parameter corresponding to each type of boundary conditions It was revealed that nonlocal elasticity theory can estimate the biaxial buckling response of SLGSs with great accuracy using the proposed values for the nonlocal parameter. which is comparable to the results of MD simulation. This analysis showed that the importance of the small length scale is dependent on the boundary conditions of SLGS.

References

[1] Ma, Q. and Clarke, D. R. , “Size dependent Hardness of Silver Single Crystals”, *Materials Research*, Vol. 10, pp. 853-63.1995.

- [2] Ebrahimi, F. Salari, E., "Thermal buckling and free vibration analysis of size dependent Timoshenko FG", *Composite Structures*, vol. 128, pp. 363-380.2015.
- [3] Murmu, T. and Pradhan, S.C., "Small-scale effect on the free in-plane vibration of nanoplates by nonlocal continuum model", *Physica E*, Volume 41, Issue 8, pp. 1628-1633.2009.
- [4] R. Ansari, S., Sahmani, "Prediction of biaxial buckling behavior of single-layered graphene sheets based on nonlocal plate models and molecular dynamics simulations", *Applied Mathematical Modelling*, Volume 37, Issues 12-13, Pages 7338-7351.2013.
- [5] S. Kitipornchai, X.Q. He, K.M. Liew, "Continuum model for the vibration of multilayered graphene sheets," *Phys. Rev. B* 72 075443.2005.
- [6] K.M. Liew, X.Q. He, S. Kitipornchai, "Continuum model for the vibration of multilayered graphene sheets," *Acta Mater.* 54 4229.2006.
- [7] R. Ansari, R. Rajabiehfard, B., Arash, B., "Nonlocal finite element model for vibrations of embedded multi-layered graphene sheets", *Computational Materials Science*, Volume 49, Issue 4, pp. 831-838.2010.
- [8] L. Shen, H.S. Shen, C.L. Zhang, "Nonlocal plate model for nonlinear vibration of single layer graphene sheets in thermal environments," *Comput. Mater. Sci.* 48 680.2010.
- [9] S.C. Pradhan, J.K. Phadikar, "Small scale effect on vibration of embedded multilayered graphene sheets based on nonlocal continuum models," *Phys. Lett. A* 373 1062.2009.
- [10] T. Murmu, S.C. and Pradhan, "Small-scale effect on the free in-plane vibration of nanoplates by nonlocal continuum model", *Physica E*, Volume 41, Issue 8, pp. 1628-1633.2009.
- [11] T. S. Narendar, S. Gopalakrishnan, "Nonlocal scale effects on wave propagation in multi-walled carbon nanotubes", *Comput. Mater. Sci.* 47 - 526.2009.
- [12] B. Arash, R. Ansari, "Evaluation of nonlocal parameter in the vibrations of single-walled carbon nanotubes with initial strain," *Physica E*, 42 - 2058.2010.
- [13] M.J. Hao, X.M. Guo, Q. Wang, Eur. J., "Small-scale effect on torsional buckling of multi-walled carbon nanotubes," *Mech. A/Solids*, 29 49.2010.
- [14] T. Natsuki, X.W. Lei, Q.Q. Ni, M. Endo, "Free vibration characteristics of double-walled carbon nanotubes embedded in an elastic medium," *Phys. Lett. A* 374 - 2670.2010.
- [15] S.K. Jang, C.W. Bert, A.G. Striz, "Application of differential quadrature to static analysis of structural components," *Int J. Num. Methods Eng.* 28, 561.1989.
- [16] R. Bellman, B.G. Kashef, J. Casti, J., "Differential quadrature: a technique for the rapid solution of nonlinear partial differential equations", *Comput. Phys.* 10, 40.1972.
- [17] A.N. Sherbourne, M.D. Pandey, "Differential quadrature method in the buckling analysis of beams and composite plates," *Comput. Struct.* 40, 903.1991.
- [18] C. Shu, "Differential quadrature and its application in engineering," *Springer*, Berlin.2000.
- [19] H.-S. Shen, C.-L. Zhang, "Postbuckling prediction of axially loaded double-walled carbon nanotubes with temperature dependent properties and initial defects", *Phys. Rev. B* 74 035410.2006.
- [20] H.-S. Shen, C.-L. Zhang, "Postbuckling of double-walled carbon nanotubes with temperature dependent properties and initial defects under combined axial and radial mechanical loads," *Int. J. Solids Struct.* 44 1461-1487.2007.
- [21] <http://lammps.sandia.gov/index.html>
- [22] W. Humphrey, A. Dalke, K. Schulten, *J. Mole. Graph.* 14 33-38.1996.
- [23] S.J. Stuart, A.B. Tutein, J.A. Harrison, "A reactive potential for hydrocarbons with intermolecular interactions" *J. Chem. Phys.* 112. 6472.2000
- [24] S.J. Stuart, A.B. Tutein, J.A. Harrison, *J. Chem. Phys.* 112, 6472.2000.
- [25] T. Natsuki, X.W. Lei, Q.Q. Ni, M. Endo, *Phys. Lett. A* 374 ,2670.2010.
- [26] K. Mylvaganam, L. Zhang, *Carbon* 42, 2025.2004.
- S. J. Miller, "The Method of Least Squares," Mathematics Department".



Computation and Simulation in Mechanical Sciences (CSMech)

Biaxial Buckling of Single-Layer Graphene Sheet Based on Nonlocal Plate Model and Molecular Dynamics Simulation

R. Pilafkan, M. Kaffash
Mirzarahimi

ORIGINAL
PAPER



Volume: 01

Issue: 02

Summer 2018

Page: 13-19

ISSN:

eISSN:

www.csmech.iaubanz.ac.ir

